Oscillatory Behavior of a Simple Kinetic Model for Proteolysis during Cell Invasion

Hugues Berry and Véronique Larreta-Garde

ERRMECE, University of Cergy-Pontoise, 95302 Cergy-Pontoise Cedex, France

ABSTRACT   Extracellular proteolysis during cell invasion is thought to be tightly organized, both temporally and spatially. This work presents a simple kinetic model that describes the interactions between extracellular matrix (ECM) proteins, proteinases, proteolytic fragments, and integrins. Nonmonotonous behavior arises from enzyme de novo synthesis consecutive to integrin binding to fragments or entire proteins. The model has been simulated using realistic values for kinetic constants and protein concentrations, with fibronectin as the ECM protein. The simulations show damped oscillations of integrin-complex concentrations, indicating alternation of maximal adhesion periods with maximal mobility periods. Comparisons with experimental data from the literature confirm the similarity between this system behavior and cell invasion. The influences on the system of cryptic functions of ECM proteins, proteinase inhibitors, and soluble antiadhesive peptides were examined. The first critical parameter for oscillation is the discrepancy between integrin affinity for intact ECM proteins and the respective proteolytic fragments, thus emphasizing the importance of cryptic functions of ECM proteins in cell invasion. Another critical parameter is the ratio between proteinase and the initial ECM protein concentration. These results suggest new insights into the organization of the ECM degradation during cell invasion.

INTRODUCTION

Cellular invasion through connective tissues is a characteristic shared by many cells during healthy (cellular immunity, wound repair, angiogenesis) or pathological (metastasis) events (Liotta et al., 1991; Price et al., 1997). Since migration is a key feature of invasion, mechanisms implied in cell migration are also applicable in cell invasion. Cells use interactions with the extracellular matrix (ECM) to move. These interactions are mainly mediated by the integrin family of transmembrane receptors, which structurally links the ECM to the cytoskeleton (Aota et al., 1991; Price et al., 1997). Integrin extracellular domains recognize different ligands of the ECM (Ruoslahti, 1988; Heino, 1996). The signal represented by integrin engagement is transmitted to the intracellular domain of this receptor (Law et al., 1996). This results in the formation of large multimolecular adhesion sites, known as focal adhesions (LaFlamme and Auer, 1996). These sites include proteins from the cytoskeleton, such as α-actinin, tensin, talin, or paxilin (Nagahara and Matsuda, 1996; Huttenlocher et al., 1996, 1997), as well as protein kinases, such as the focal adhesion kinase, or the Src family (Yamada, 1997; Tamura et al., 1998). Integrins also trigger activation of signal transduction pathways, such as lipid second messengers (Protein Kinase-C pathway) (Defilippi et al., 1997), or the mitogen-activated protein kinase and Ras pathway (Klemke et al., 1997; Schlaepfer and Hunter, 1997). In addition, the affinity of integrins for their extracellular ligands can be regulated by intracellular

signals, in a process called inside-out signaling (Yamada, 1997). Integrin signaling thus regulates cell proliferation, differentiation, survival, and adhesion (LaFlamme and Auer, 1996; Assoian, 1997). Cell migration depends on the organization of these integrin-activated pathways, but also on the asymmetry between the rear and the front of the cell in the spatial distribution of adhesion-receptor (DiMilla et al., 1991; Lauffenburger, 1996).

The ECM, being composed of a dense mesh of various insoluble proteins, constitutes both a barrier separating organisms into tissue compartments and a substratum for cell adhesion (Ruoslahti, 1988). In addition to being able to migrate, invasive cells must degrade ECM proteins to traverse connective tissues. But, because mobility requires both adhesion and detachment from the ECM (Heino, 1996), intensive matrix degradation would remove the substratum for cell adhesion and prevent mobility. Hence, it is thought that proteolysis during invasion must be highly organized, both temporally and spatially (Basbaum and Werb, 1996; Werb, 1997).

The cellular origin of the involved proteinases is still unclear. Some of them are produced directly by the invasive cells, and are partly responsive for localized proteolysis, which has been shown to be necessary for invasion (Nakahara et al., 1997; Werb, 1997). Invasive cells can also recruit surrounding stromal cells to produce proteinases (Basbaum and Werb, 1996; Borchers et al., 1997; Guo et al., 1997). The proteinases are then thought to migrate to the invasive cell membrane, where they can bind to specific receptors (Yebra et al., 1996) or to molecules acting as receptors, such as membrane-type proteinases or integrins (Brooks et al., 1996). However, interactions between invasive cell integrins and the ECM can itself induce overexpression of extracellular proteinase genes in the invasive cell (Khan and Falcone, 1997; Sudbeck et al., 1997). Fur-

thermore, this upregulation enhances melanoma cell invasion in vitro (Bafetti et al., 1998).

The participants in the interplay of matrix proteolysis and cell adhesion are now well characterized. Excreted or membrane-bound matrix metalloproteinases (MMPs) constitute the main proteinase family involved (for reviews see Birkedal-Hansen et al., 1993 and Hulboy et al., 1997), but others such as the plasminogen/plasminogen activator pair also play an important role (Vassali and Pepper, 1994). However, the mechanisms by which this system could be properly organized in vivo to satisfy the criteria necessary for invasion are poorly understood.

A realistic model for cell invasion should thus include the different origins and specificities of the proteinases implied. Furthermore, it should include the mechanisms involved in cell migration, presented above. Unfortunately, the number of events triggered by integrin engagement are increasingly numerous, and the molecular mechanisms involved are mostly unknown (LaFlamme and Auer, 1996; Yamada, 1997).

In this work, we propose a simple model based only on a kinetic description of the proteinase-mediated ECM degradation to test the hypothesis that such a simple molecular model could give rise to an organized system. Hence, the aim of this study is not to build a realistic model for cell invasion, but to address the possibility that extracellular proteolysis could, by itself, become organized, thus excluding other interactions or pathways that necessarily also play an important role in cell invasion.

Nonmonotonous behaviors (thresholds, oscillations, self-organization or chaos) originating from simple kinetic models have been observed both theoretically and experimentally. Nonlinearity in such systems can arise from negative or positive feedback (Goldbeter and Martiel, 1985; Goldbeter et al., 1988; Goldbeter and Guilmot, 1996), substrate cycling (Coevoet and Hervagault, 1997), allosteric regulation (Mikhailov and Hess, 1996), or sensibility to environmental factors (Bronnikova et al., 1998). In our model, nonlinearity originates from proteinase neosynthesis due to enzyme substrate and/or product binding to integrins. Such a neosynthesis in response to cell binding to ECM components has been shown experimentally by many authors (Werb et al., 1989; Homandberg et al., 1997; Khan and Falcone, 1997; Sudbeck et al., 1997; Bafetti et al., 1998). We especially focused on the role of the cryptic functions displayed by ECM proteins. These functions are not observed in the intact protein, but are expressed by respective proteolytic fragments, and are hypothesized to play a role in ECM proteolysis organization (Fukai et al., 1995; Ugarova et al., 1996; Gianelli et al., 1997). The theoretical results simulated here are discussed in light of recently published experimental data.

CONSTRUCTION OF THE MODEL

Presentation and rate expression

The model (Fig. 1) kinetically expresses the action of an extracellular proteinase (E) catalyzing the proteolysis of an
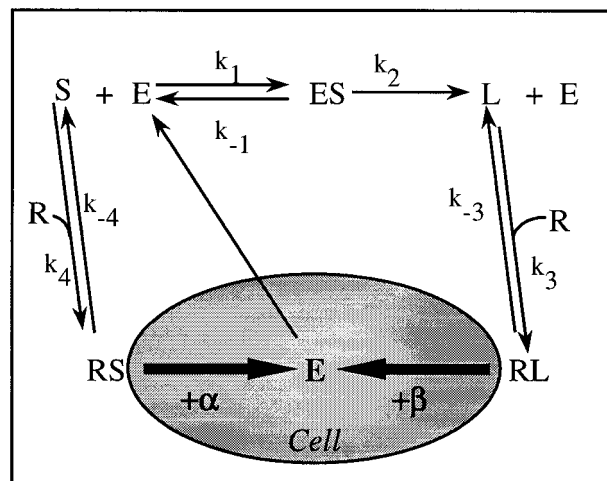

FIGURE 1 Proposed kinetic scheme for proteolysis organization during cell invasion. E, proteinase; S, intact ECM protein; L, proteolytic fragment from S degradation by E; R, integrin (membrane-bound) receptor; RS, membrane-bound complex formed with integrin and intact ECM protein; RL, membrane-bound complex formed with integrin and ECM protein fragment; α, coefficient for proteinase neosynthesis consecutive to RS complex formation; β, coefficient for proteinase neosynthesis consecutive to RL complex formation.

ECM protein (S), through a single enzyme substrate complex (ES). S can also reversibly bind to an integrin receptor (R) on the cell surface, resulting in the RS complex (dissociation constant $K_D^S = k_{-4}/k_4$). One product of S proteolysis, designated as L, is also assumed to bind to the integrin (RL complex), possibly with a different dissociation constant ($K_D^L = k_{-3}/k_3$).

In this model, both S and L association with R can give rise to proteinase neosynthesis. We assume here a simple relationship between the proteinase concentration that is synthesized de novo after the formation of complexes with R, that is, $[E]_{neosynthesis} = \alpha[RS] + \beta[RL]$. Thus the quantities α and β represent the quantitative response of integrin engagement, resulting in proteinase gene expression. For example, in rabbit synovial fibroblasts, binding of fibronectin (Fn) fragments to integrins induces collagenase and stromelysin upregulation, whereas binding of entire Fn does not (Vassali and Pepper, 1994). This would correspond here to $\alpha = 0$ and $\beta > 0$. Similarly, the formation of complexes between entire vitronectin and integrins in melanoma cells induces metalloproteinase expression, whereas those of corresponding vitronectin fragments do not (Bafetti et al., 1998). This situation could be approached here by $\alpha > 0$ and $\beta = 0$. Engagement of integrins by different Fn fragments can trigger metalloproteinase upregulation or inhibit this upregulation, depending on the fragment (Huhtala et al., 1995). Thus α and β can be set to positive or negative values. Of course, realistic values of α and β are expected to be variable, depending on cell type, differentiation state, focal adhesion formation, expressed integrin signaling pathways, and other factors.

For simplification, we have considered only constant values of α and β. Although oversimplifying, this approach

allows simulating cryptic functions of the proteolytic fragments (i.e., $\alpha \neq \beta$). Thus, as $[E]_{neosynthesis}$ becomes a simple linear function of [RS] and [RL], the time derivative of the de novo-synthesized enzyme concentration, can be expressed as $\partial([E]_{neosynthesis})/\partial t = \alpha(\partial[RS]/\partial t) + \beta(\partial[RL]/\partial t)$. This term is added to the classical rate of change of enzyme concentration, corresponding to enzyme catalysis $(\partial([E]_{catalysis})/\partial t = ((k_{-1} + k_2)[ES]) - k_1[E][S])$, to obtain the global rate of change expressed in Eq. 3.

As S is part of the ECM, RS complex formation locally enhances the force cells must apply to detach themselves from the ECM (DiMilla et al., 1991; Palecek et al., 1997). High [RS] values would thus hinder cell mobility, and can be considered as pro-adhesive. S proteolysis is assumed to extract (solubilize) the resulting fragment, L, from the ECM. L molecules are not bound to the ECM, so that RL complexes are detached from it. [RL] values can thus be considered as pro-mobile, in the sense that RL complexes locally enhance cell detachment capacity. The cell's overall capacity to move at a given time was thus approached here as the balance between the [RL] and [RS] values at this time.

Enzyme kinetics have been solved without steady state or rapid equilibrium assumptions, thus allowing large variations in $[E]_0/[S]_0$. The ordinary differential equations describing this system are

$$\frac{\partial[S]}{\partial t} = \overbrace{k_{-1}[ES] - k_1[E][S]}^{\text{proteolysis}}$$
$$+ \overbrace{k_{-4}[RS] - k_4[S]([R]_0 - [RS] - [RL])}^{\text{integrin binding}}, \quad (1)$$

$$\frac{\partial[L]}{\partial t} = \overbrace{k_2[ES]}^{\text{proteolysis}}$$
$$+ \overbrace{k_{-3}[RL] - k_3[L]([R]_0 - [RS] - [RL])}^{\text{integrin binding}}, \quad (2)$$

$$\frac{\partial[E]}{\partial t} = \overbrace{(k_{-1} + k_2)[ES] - k_1[E][S]}^{\text{proteolysis}}$$
$$+ \overbrace{\alpha\frac{\partial[RS]}{\partial t} + \beta\frac{\partial[RL]}{\partial t}}^{\text{enzyme neo-synthesis}}, \quad (3)$$

$$\frac{\partial[ES]}{\partial t} = \overbrace{-(k_{-1} + k_2)[ES] + k_1[E][S]}^{\text{proteolysis}}, \quad (4)$$

$$\frac{\partial[RL]}{\partial t} = \overbrace{-k_{-3}[RL] + k_3[L]([R]_0 - [RS] - [RL])}^{\text{integrin binding}}, \quad (5)$$

$$\frac{\partial[RS]}{\partial t} = \overbrace{-k_{-4}[RS] + k_4[S]([R]_0 - [RS] - [RL])}^{\text{integrin binding}}, \quad (6)$$

where $[R]_0 = [R] + [RL] + [RS]$.

This set of differential equations has been numerically integrated and solved using a solver specific for stiff equations (ODE23s) with MATLAB 5.0 (Math Works Inc., Natick, MA) on a personal computer.

Kinetic constant and initial concentration values

For simulation purposes, realistic values of kinetic constants and initial concentrations were chosen, using Fn as substrate (S). Fn is an ECM glycoprotein that plays a key role in ECM assembly and cell adhesion (for a review, see Ruoslahti, 1988).

The main difficulty for defining realistic concentration values are, for one part, the absence of quantitative values in the literature, but also the possibility of diffusion-limited reaction rates or nonhomogeneous concentration distributions due to low diffusion constants in the ECM. To overcome this difficulty, we have varied each concentration over wide ranges, hypothesizing that realistic values at any distance from the cell would be in these large intervals. Of course, this oversimplifying approach does not allow the identification of possible mechanisms of spatial pattern formation, which are often observed in diffusion-reaction systems (Murray, 1993).

Enzyme kinetic constant values were evaluated based on studies of plasma Fn proteolysis by thermolysin, a bacterial metalloproteinase, commonly used as a model for MMPs (Berry and Larreta-Garde, unpublished results). Assuming $k_2 \ll k_{-1}$, the values were set to $k_1 = 10^8 \text{ M}^{-1} \cdot \text{s}^{-1}$, $k_{-1} = 1.4 \times 10^4 \text{ s}^{-1}$, and $k_2 = 110 \text{ s}^{-1}$.

Affinity constants for integrin binding were taken from the literature. The $\alpha_5\beta_1$ integrin dissociation constant for Fn was evaluated at 8×10^{-7} M (Akiyama and Yamada, 1985), but can vary from 4×10^{-8} (McKeown-Longo and Mosher, 1988) to $>10^{-6}$ M (Wu, 1997), depending on cell type. Furthermore, some Fn proteolytic fragments show increased affinity compared to the entire molecule (Akiyama et al., 1985; Xie and Homandberg, 1993). Dissociation constants in this study were thus varied between 10^{-6} and 10^{-8} M.

Initial concentrations primarily depend on the considered volume. Here it was defined as the average ECM volume surrounding a stroma cell. Values of cell density in interstitial stroma are not available in the literature, but observations of human superficial dermis allow an estimation of this density at 2000 to 5000 fibroblasts/mm^3 ECM, after corrections of volume variations caused by tissue preparation (G. Godeau, unpublished results). This corresponds to a value of 2 to 5×10^{-10} L ECM/fibroblast.

The choice of an average ECM volume around the stromal cell as reference volume, can appear arbitrary. Furthermore, cell density in the ECM itself varies, depending on

the ECM type considered. However, the choice of large ranges for concentration variations should encompass most of the cases encountered in vivo, so that the results presented here can be considered as independent of cell density or effective volume.

The quantity of Fn cell surface receptors has been evaluated at 10^5 to 5×10^5 receptors/cell (Akiyama and Yamada, 1985; Akiyama et al., 1985). Considering the volume determined above, $[R]_0$ values varied here between 20 pM and 200 nM.

Most studies on MMP regulation use qualitative values such as those obtained from northern blots. To our knowledge, the only available quantitative values range from 10^4 (Yebra et al., 1996) to 10^8 (Homandberg et al., 1997) proteinases/cell, resulting in an initial enzyme concentration of 1 pM $\leq [E]_0 \leq$ 800 nM.

Human triple helical collagen is a 3000-Å-long molecule composed of approximately 3000 amino acids (Linsenmayer, 1983). The internal collagen concentration at sol-gel transition can thus be estimated at roughly 100 g/L, as evaluated by overlap concentration C* (de Gennes, 1993). Fn concentration varies with ECM types, but usually falls between 1 and 3% (Hynes, 1983). Assuming that ECM is almost exclusively composed of collagen (in mass), Fn concentration in ECM has been assumed to range from 20 nM to 20 μM.

RESULTS

Influence of dissociation constants for integrin–ligand complexes

Even with $\alpha = \beta$, i.e., excluding differential neosynthesis conditions, damped oscillations of [RL], [RS], and [E] appear (Fig. 2). [RL] and [RS] oscillations are 180° out of phase, whereas [E] local maxima correspond to those of [RL]. As oscillation periods are not constant, here we define the period for each local maximum as the difference between the time corresponding to the local maximum considered and that corresponding to the former local maximum.

Inasmuch as invasion necessitates both cell adhesion to the ECM and detachment from it, a behavior where RL and RS concentrations would monotonically reach equilibrium would favor cell adhesion or detachment (depending on the highest value of RL or RS at equilibrium), but not invasion. By considering RL complexes as pro-mobile and RS complexes as pro-adhesive for the cell (DiMilla et al., 1991; Lauffenburger, 1996; Palecek et al., 1997), the oscillations observed here would induce periods of maximal adhesion (minimal mobility) in alternation with periods of maximal mobility (minimal adhesion). In each case, the oscillation damping finally results in stable points where $dC_i/dt = 0$ (where C_i represents any species concentration). We have verified that these final points are asymptotically stable: each eigenvalue of the Jacobian matrix at these points has strictly negative real parts (Porter, 1967).
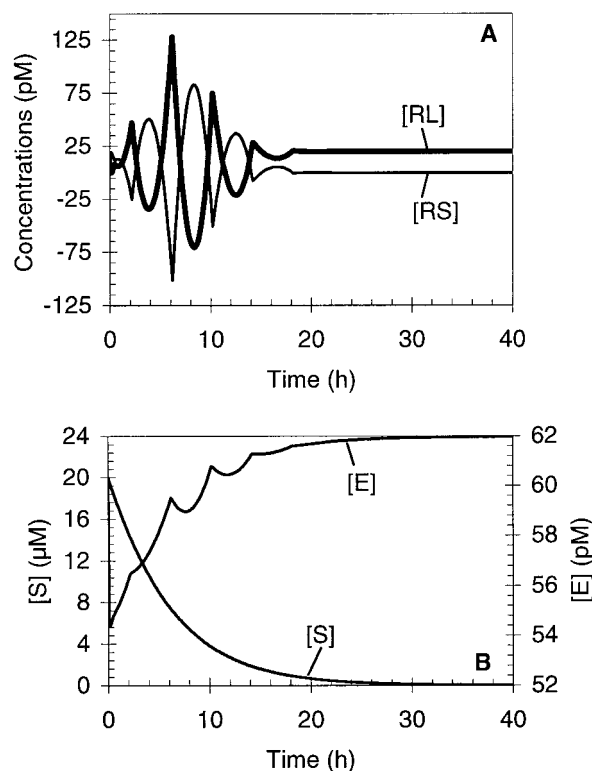

FIGURE 2 Simulation of (A) [RL] and [RS] or (B) [S] and [E] variations with $K_D^S/K_D^L = 100$ and $\alpha = \beta = 0.1$. $K_D^S = 10^{-6}$ M; $K_D^L = 10^{-8}$ M; $[E]_0 = 60$ pM; $[S]_0 = 20$ μM; $[R]_0 = 20$ pM.

Oscillation periods vary between 0.5 and 4 h for $K_D^S/K_D^L = 100$ (Fig. 3). Assuming a cell dimension in the direction of invasion of 10 μm, and that one oscillation period allows a cell movement of 0.25 to 1 times its length, cell invasion speed would be of the order of 0.75 to 20 μm $\cdot$ h^{-1}.

The discrepancy between K_D^S and K_D^L values relates to cryptic functions of ECM proteins. Both oscillation amplitude and period depend on the ratio K_D^S/K_D^L. For $\alpha = \beta = 0.1$, oscillations are observed when $K_D^S/K_D^L > 3$ (Fig. 3). For

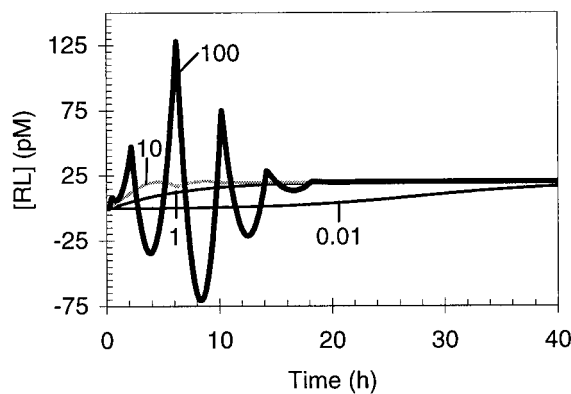
FIGURE 3 [RL] oscillations as a function of K_D^S/K_D^L. The numbers indicated represent the values of K_D^S/K_D^L used for each simulation. $\alpha = \beta = 0.1$; $[E]_0 = 60$ pM; $[S]_0 = 20$ μM; $[R]_0 = 20$ pM.

higher values corresponding to more accentuated cryptic functions, the oscillation amplitude increases and periods decrease with increasing K_D^S/K_D^L. Oscillations appear when the discrepancy between K_D^S/K_D^L is higher than a threshold value of the ratio K_D^S/K_D^L. For clarity purposes, this critical value of K_D^S/K_D^L will be referred to here as ρ_c. As will be seen below, ρ_c largely depends on α and β.

In Fig. 2 B, [E] variations result from two influences, as described by Eq. 3. The global shape of [E] evolution corresponds to a classical hyperbolic kinetic evolution. This can be considered to represent the catalytic terms of Eq. 3 $((k_{-1} + k_2)[ES] - k_1[E][S])$. Added to this global shape, oscillations related to the de novo synthesis terms of Eq. 3 $(\alpha(\partial[RS]/\partial t) + \beta(\partial[RL]/\partial t))$ appear. When proteinase gene expression resulting from integrin engagement is not amplified, i.e., one ligand-integrin complex formation produces less than one enzyme molecule (α and/or $\beta \in 1$), the kinetic component prevails and [E] variations show a global hyperbolic shape (Fig. 2 B). Nevertheless, with increasing α and/or β, i.e., amplifying conditions, the periodic behavior prevails, and the global shape of [E] variations tends to be purely oscillating (data not shown). Amplification of integrin engagement by signal transduction pathways could thus be of importance in extracellular proteinase activity oscillations.

Influence of α and β

The influence of α and β values on the appearance of the oscillations was approached by evaluating the minimal value of the ratio K_D^S/K_D^L that allows oscillations (ρ_c). To limit the α and β variation ranges, we have simulated two different situations. In a first approach, we have varied the overall level of de novo synthesis (i.e., $\alpha + \beta$), through variations of a single parameter (i.e., α varies and $\beta = 0$, or β varies and $\alpha = 0$). In this case (Fig. 4 A), ρ_c depends on α or β in similar ways, whenever α or $\beta = 0$. ρ_c is found to be minimal for α or β values between 3 and 4. Note that, for such optimal values, ρ_c can be as low as 2. This means that discrepancies between integrin affinity for an entire ECM protein and related fragments that would yield $K_D^S/K_D^L = 2$ could be sufficient for the oscillations to appear. Moreover, ρ_c increases for $\alpha + \beta$ values different from these optimal values, even when α (or β) < 0. Another interesting case is the situation where RS and RL complexes have exactly opposite effects on signal transduction (i.e., $\alpha = -\beta$: the overall level of de novo synthesis is unchanged). In this case (Fig. 4 B), ρ_c presents a minimal value at $\alpha = -\beta \approx 2$. Under these conditions, the oscillation appearance seems favored when RS complexes slightly enhance proteinase expression, but would be less favored when RS-mediated proteinase overexpression is higher or when RS complexes inhibit proteinase expression. Taken together, the results presented in Fig. 4 suggest that the minimal value of K_D^S/K_D^L that allows oscillations could depend on the modalities of integrin transduction pathways.

To observe the influence of α and β on the oscillation shape without changes in global neosynthesis, the $\alpha + \beta$
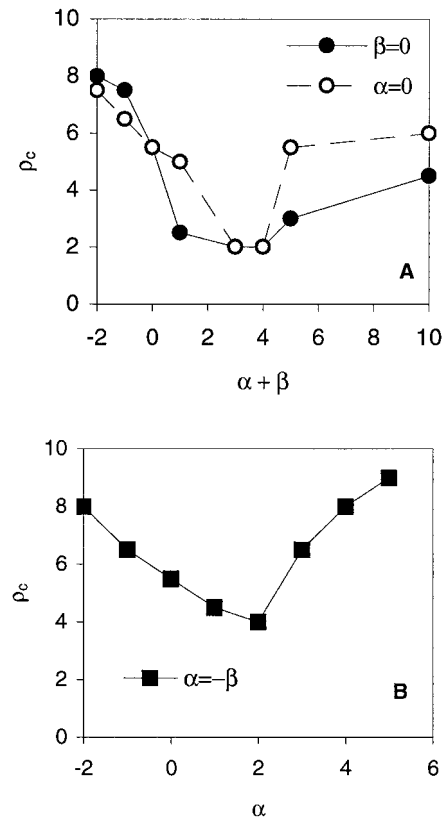

FIGURE 4 Dependence of ρ_c on α and β. ρ_c represents the minimal K_D^S/K_D^L value that allows oscillatory behaviors to appear. (A) Variation of the overall level of de novo synthesis ($\alpha + \beta$), with $\beta = 0$ (●) or $\alpha = 0$ (○). (B) Variations of α under constant level of de novo synthesis ($\alpha = -\beta$) (■).

value was kept constant while varying α. We have simulated two kinds of situations: when $\alpha = \beta$, L and S participate equally in enzyme neosynthesis. Cryptic functions are introduced by using $\alpha = 0$ (only RL complexes are responsible for enzyme neosynthesis) or $\alpha < 0$ (enzyme neosynthesis is induced by RL and inhibited by RS). When $K_D^S/K_D^L > \rho_c$, the modification of cryptic functions does not change the overall shape of the oscillations, but considerably decreases both their amplitude and periods (Fig. 5). The qualitative behavior of the system is almost identical whether $\alpha = 0$ or $\alpha < 0$. Thus, the value of α or β (i.e., the extent of the integrin signal amplification by transduction pathways) does not appear crucial for the system, as soon as $K_D^S/K_D^L > \rho_c$.

Influence of $[E]_0/[S]_0$

$[E]_0/[S]_0$ is an important parameter of the system, because it defines, together with K_D^L and K_D^S, the characteristic time of L and S variation. Indeed, as seen in Fig. 6, oscillation appearance clearly depends on $[E]_0/[S]_0$. The system is oscillatory for $[E]_0/[S]_0 \leq 0.3$ and [RL] and [RS] almost immediately reach equilibrium for higher values. For high $[E]_0/[S]_0$ values, S reaches equilibrium too rapidly, com-
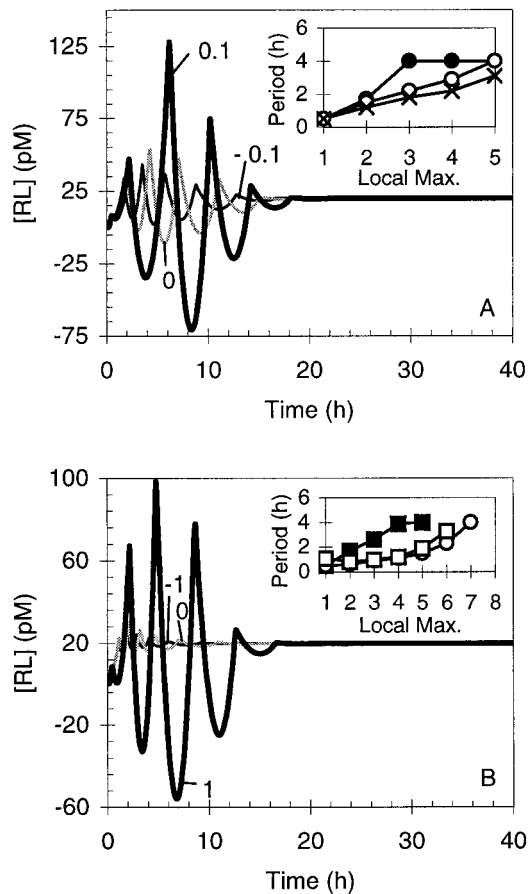
FIGURE 5   [RL] oscillations as a function of α, with $\alpha + \beta = 0.2$ (A) or 2.0 (B). The numbers indicated represent the values of α used for each simulation. $K_D^S = 10^{-6}$ M; $K_D^L = 10^{-8}$ M; $[E]_0 = 60$ pM; $[S]_0 = 20$ μM; $[R]_0 = 20$ pM. *Inserts:* Corresponding period evolutions of the local maxima for $\alpha = 0.1$ (●), 0 (○), -0.1 (×), 1 (■), or -1 (□). Periods are defined as in text.

pared to K_D^L and K_D^S, to allow oscillations to occur. The oscillatory behavior would thus be a function of the ECM composition (i.e., substratum concentration in the ECM), but also of the basal level of proteinase excreted.
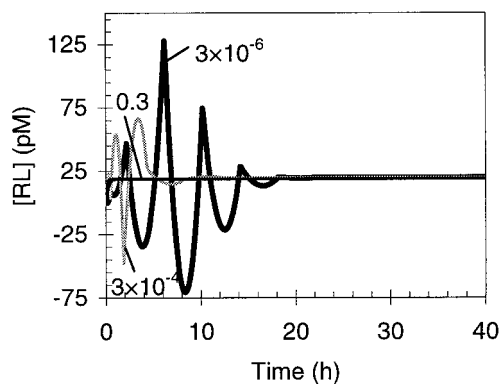

FIGURE 6   [RL] oscillations as a function of $[E]_0/[S]_0$. The numbers indicated represent the values of $[E]_0/[S]_0$ used for each simulation. $\alpha = \beta = 0.1$; $K_D^S = 10^{-6}$ M; $K_D^L = 10^{-8}$ M; $[R]_0 = 20$ pM.

Influence of $[R]_0$

The influence of global integrin concentration on the system depends on $[S]_0$. For high $[S]_0$ values (Fig. 7 A), oscillation periods and amplitude decrease with increasing $[R]_0$. Under these conditions, [RL] variations are oscillatory for $[R]_0 < 200$ nM. At low $[S]_0$ values (Fig. 7 B), $[R]_0$ has an opposite effect: [RL] variations are oscillatory if $[R]_0 > 200$ nM. The $[R]_0$ effect is thus biphasic: increasing $[R]_0$ values promote oscillations at low $[S]_0$, but inhibit them at high $[S]_0$. These simulations predict a biphasic influence of integrin concentration on oscillations, which depends on substrate concentration: increasing global integrin concentration promotes oscillations at low substrate concentrations, but inhibits them at high concentrations. In terms of cell movement, this implies that the influence of integrin expression in invasion could depend on ligand concentration in the ECM.

Influence of an enzyme inhibitor

A competitive enzyme inhibitor similar to those encountered in vivo or to artificial ones (Birkedal-Hansen et al., 1993) was introduced in the model. K_i values for these inhibitors vary approximately between 0.1 and 70 nM
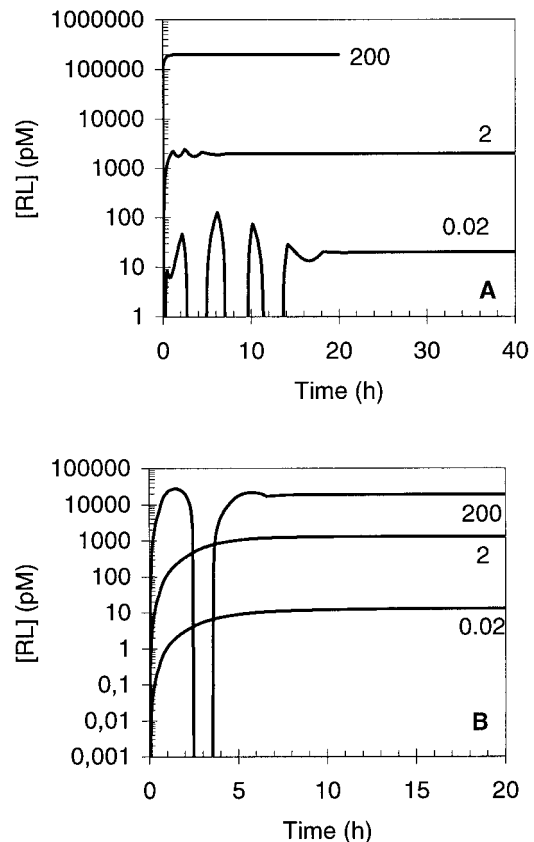

FIGURE 7   [RL] oscillations as a function of $[R]_0$ with (A) high ($[S]_0 = 20$ μM) or (B) low ($[S]_0 = 20$ nM) $[S]_0$ values. The numbers indicated represent the values of $[R]_0$ (nM) used for each simulation. $\alpha = \beta = 0.1$; $K_D^S = 10^{-6}$ M; $K_D^L = 10^{-8}$ M; $[E]_0 = 60$ pM.

(Birkedal-Hansen et al., 1993; Hynes, 1983; Taylor et al., 1996). Here we chose a K_i (= k_{-5}/k_5) value of 10 nM ($k_{-5} = 10^{-4}$ s^{-1}; $k_5 = 10^4$ M$^{-1} \cdot$ s^{-1}).

In this case, the system of ordinary differential equations (Eqs. 1–6) is slightly modified, Eq. 3 being replaced by

$$\frac{\partial[E]}{\partial t} = (k_{-1} + k_2)[ES] - k_1[E][S] + \alpha \frac{\partial[RS]}{\partial t} + \beta \frac{\partial[RL]}{\partial t}$$
$$+ k_{-5}([I]_0 - [I]) - k_5[E][I]. \quad (7)$$

A new variable, [I] (inhibitor concentration), is introduced, as well as its accompanying differential equation,

$$\frac{\partial[I]}{\partial t} = k_{-5}([I]_0 - [I]) - k_5[E][I], \quad (8)$$

where $[I]_0 = [I] + [EI]$.

The simulations in Fig. 8 clearly show a decrease in oscillation amplitude for $[I]_0 > 10$ nM. A period increase is observed for $[I]_0 > 50$ nM (Fig. 8, *insert*). Oscillations totally disappear for $[I]_0 \geq 0.5$ μM (data not shown).

Influence of a soluble integrin ligand

We have also introduced soluble integrin ligands, similar to arginine-glycine-aspartic acid (RGD) peptides, which act as competitors of L and S binding to R, without involvement of proteinase neosynthesis. Such peptides show K_D values for integrin binding between 10^{-12} and 10^{-9} M (Xiao and Truskey, 1996). Here, the K_D value (= k_{-6}/k_6) has been set to 1 nM ($k_{-6} = 10^{-4}$ s^{-1}, $k_6 = 10^5$ M$^{-1} \cdot$ s^{-1}).

The system of differential equations (Eqs. 1–6) is changed, with Eqs. 1, 2, 5, and 6, replaced, respectively, by

$$\frac{\partial[S]}{\partial t} = k_{-1}[ES] - k_1[E][S] + k_{-4}[RS]$$
$$- k_4[S]([R]_0 - [RS] - [RL] - [RP]), \quad (9)$$

$$\frac{\partial[L]}{\partial t} = k_2[ES] + k_{-3}[RL]$$
$$- k_3[L]([R]_0 - [RS] - [RL] - [RP]), \quad (10)$$

$$\frac{\partial[RL]}{\partial t} = -k_{-3}[RL] + k_3[L]([R]_0 - [RS] - [RL] - [RP]), \quad (11)$$

$$\frac{\partial[RS]}{\partial t} = -k_{-4}[RS] + k_4[S]([R]_0 - [RS] - [RL] - [RP]), \quad (12)$$

Here again, a new variable, [RP] (peptide–integrin complex concentration), is introduced, as well as its accompanying differential equation,

$$\frac{\partial[RP]}{\partial t} = k_6([P]_0 - [RP])([R]_0 - [RS] - [RL] - [RP])$$
$$- k_{-6}[RP], \quad (13)$$

where $[P]_0$ is the global RGD peptide concentration ($[P]_0 = [P] + [RP]$) and $[R]_0 = [R] + [RL] + [RS] + [RP]$.

With increasing peptide concentrations, a slight decrease in oscillation amplitude is observed (Fig. 9). However, in contrast to the behavior observed with increasing enzyme inhibitor concentrations, the simulations do not show any modification of the period (Fig. 9, *insert*). Moreover, such peptides are less crucial as far as oscillatory behaviors are concerned, since oscillations disappear only with $[P]_0 > 1$ μM.

DISCUSSION

Comparison to experimental data

Although the process of cell migration is still unclear, integrin engagement, subsequent organization of the cy-
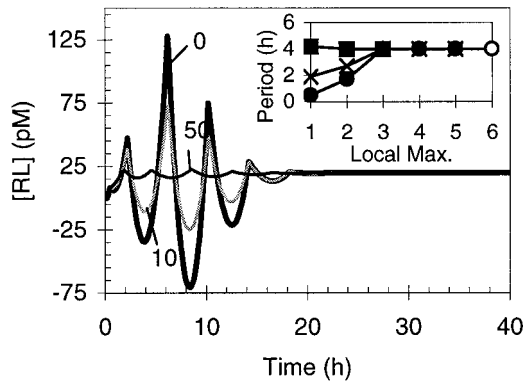

FIGURE 8 [RL] oscillations as a function of a proteinase inhibitor I. The numbers indicated represent the values of $[I]_0$ used for each simulation (nM). $\alpha = \beta = 0.1$; $K_D^S = 10^{-6}$ M; $K_D^L = 10^{-8}$ M; $K_i = 10^{-8}$ M; $[E]_0 = 60$ pM; $[S]_0 = 20$ μM; $[R]_0 = 20$ pM. *Insert:* Corresponding period evolutions of the local maxima for $[I]_0 = 0$ (●), 10 (○), 50 (×), or 100 (■) nM. Periods are defined as in text. Data series for $[I]_0 = 0$ and 10 nM are superimposed.
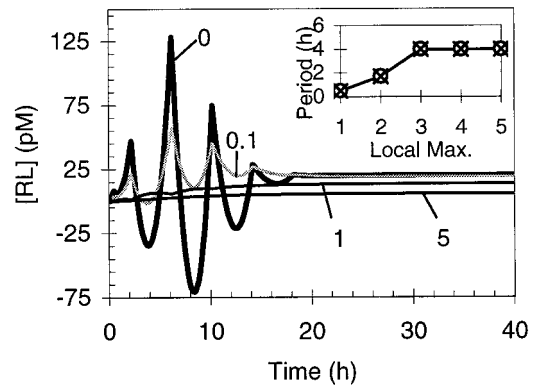
FIGURE 9 [RL] oscillations as a function of a soluble RGD peptide, P. The numbers indicated represent the values of $[P]_0$ used for each simulation (μM). $\alpha = \beta = 0.1$; $K_D^S = 10^{-6}$ M; $K_D^L = 10^{-8}$ M; $K_D = 10^{-9}$ M; $[E]_0 = 60$ pM; $[S]_0 = 20$ μM; $[R]_0 = 20$ pM. *Insert:* Corresponding period evolutions of the local maxima for $[P]_0 = 0$ (●), 0.01 (○), or 0.1 (×) μM. Periods are defined as in text. All data series are superimposed.

toskeleton, and integrin signaling are known to be involved (Nagahara and Matsuda, 1996; Huttenlocher et al., 1996; Tamura et al., 1998). The purpose of our work is not to present a true realistic model for cell invasion, since the complexity and diversity of the implied molecular interactions (when known) do not allow such an attempt. We have focused our attention on the main difference between cell migration and invasion, i.e., the requirement for the invasive cell to degrade the ECM it crosses. Under certain conditions, the simple kinetic model presented here shows a damped oscillatory behavior of RL, RS, and E concentrations, during which RL and RS are 180° out of phase. These oscillations would induce periods of maximal adhesion (minimal mobility) in alternation with periods of maximal mobility (minimal adhesion).

Consistent with our results, the existence of pericellular proteolysis oscillations has recently been observed experimentally during neutrophil migration over artificial matrices (Kindzelskii et al., 1998). The period of these oscillations (≈ 20 s) was shorter than those inferred from our theoretical results. Nevertheless, despite the fact that space is not represented in our model, the present work deals with cell invasion (motility inside an ECM volume), whereas the cited work studied surface migration (motility above two-dimensional ECM surfaces). This discrepancy between oscillation periods could also be due to diffusion phenomena, as mentioned above. Our results furthermore show that extracellular proteolysis oscillations could be related to the amplification of integrin engagement (α and β values) by the signal transduction pathways that lead to proteinase gene expression. However, further information about the molecular mechanisms involved in integrin signaling are required to determine the in vivo relevance of this parameter.

Our model predicts cell migration speeds varying from 0.75 to 20 μm $\cdot$ h^{-1}. This range is in very good agreement with previously reported experimental values (from 1 to 20 μm·h^{-1}; Palecek et al., 1997). Moreover, the biphasic influence of the integrin concentration on migration has been observed experimentally for cell migration (Huttenlocher et al., 1996; Palecek et al., 1997). Hence, the features of extracellular proteolysis organization during cell invasion, as predicted from the present theoretical work, seem qualitatively consistent with those observed and predicted for cell migration.

Crucial parameters

A major argument in favor of theoretical models, such as the one presented here, is that they allow discerning parameters that are crucial for the observed behavior, among a large number of intervening ones. The most crucial parameters for the appearance of oscillatory behavior in the system are the characteristic time of L and S variation, as well as the cryptic functions of the ECM protein considered. The first parameter primarily depends on the initial concentration ratio, $[E]_0/[S]_0$. Oscillations appear for low values of this

ratio, and progressively disappear as it increases. For low substratum concentration ranges, cell migration speed experimentally increases with increasing adhesion substratum concentrations (Palecek et al., 1997). Furthermore, it is known that, in some cases, some MMPs could be too active in ECM degradation to efficiently mediate cell invasion (Cockett et al., 1998).

Cryptic functions of ECM proteins have been implicated in many events governed by cell–ECM interactions, such as differentiation (Fukai et al., 1993, 1995), adhesion (Fukai et al., 1996; Ugarova et al., 1996), migration (Fukai et al., 1995; Gianelli et al., 1997), and MMP regulation (Bafetti et al., 1998; Werb et al., 1989). The results presented in this work suggest that cryptic functions would also play a key role in proteolysis organization during invasion. Oscillations appear only when the ratio K_D^S/K_D^L is higher than a threshold value ρ_c that, in turn, depends on the modalities of integrin transduction pathways. It is notable that the oscillations can appear as soon as the integrin affinity for the ECM protein fragment is higher or equal to twice that for the entire protein. Moreover, our results suggest that, for a given value of K_D^S/K_D^L, the oscillations could appear (or disappear) with varying cellular response to integrin binding. Thus, the regulation of integrin transduction pathways as a function of the composition of the ECM encountered (and corresponding cryptic activities) could be important in cell invasion.

Enzyme inhibitors and soluble RGD peptides

Introduction of enzyme inhibitors and soluble RGD peptides provides further validation of the model. The disappearance of oscillations at high inhibitor or soluble peptide concentrations confirms the importance of the interplay of enzyme proteolysis and interactions with integrins in oscillatory behavior. Moreover, the model presented here suggests a difference in the way proteinase inhibitors or RGD peptides act on cell invasion. RGD peptides would enhance detachment of invasive cells from the ECM, whereas proteinase inhibitors would decrease cell speed (oscillation periods increase). Furthermore, the proteinase inhibitor concentration that allows disappearance of oscillation is much lower than the corresponding RGD peptide concentration. These data suggest that proteinase inhibitors could be more powerful inhibitors of cell invasion than are adhesion inhibitors. This result could be related to clinical studies that have demonstrated that MMP inhibitors are potential anti-metastatic agents (Denis and Verweij, 1997).

Confidence in the numerical analysis

Considering the relative complexity of the model presented here, a numerical-only approach was undertaken. Nevertheless, some analytical remarks can be made. First, the model (Eqs. 1–6) can be simplified by noting that $[ES] + [E] - \alpha[RS] - \beta[RL] = [E]_0$, and $[E] - [S] - [L] -$

$(\alpha + 1)[RS] - (\beta + 1)[RL] = [E]_0 - [S]_0$. This allows one to reduce the differential equation set to four equations, but dramatically complicates the corresponding right-hand terms (up to 20 different components). This procedure reveals terms in $[RL]^2$ and $[RS]^2$, that could account for the dynamic behavior observed. Moreover, periodic solutions are often observed in simple physical systems containing first- and second-order time derivatives (Sobolev, 1989). The system presented here could not be re-arranged to express second-order time derivatives for [RL] and [RS]. However, because the rates of change of each species are closely interrelated, such a possibility cannot be completely excluded.

Other mechanisms involved in cell invasion

A large number of mechanisms are thought to be important for cell invasion. Whereas the present study only deals with extracellular proteolysis organization, many other intervening phenomena have been ignored. The model presented here is thus to be considered as a basis for the building of better models, implying further phenomena. Some of these present an autocatalytic nature that could enhance the dynamical characteristics of the model presented here (instability). This is the case of pro-MMP activation or of the coupling between haptotaxis and mechanical cell traction (Cook et al., 1993). MMP localization on cell surface receptors could also play an important role by enhancing local proteinase concentrations, and modifying the MMP/inhibitor local balance (Liotta et al., 1991). This has been accounted for in the model presented here by modifying initial proteinase concentrations. Whether the proteinases used by invasive cells to degrade the ECM are produced by these cells themselves, or recruited from surrounding stromal cells, is still unclear. Both possibilities seem to be involved in vivo (Basbaum and Werb, 1996; Bafetti et al., 1998). The present study deals only with the first one, but both of them should be included in a more realistic model. A lack of information about the corresponding diffusion processes (nature and diffusion coefficient of diffusing species, relative importance of both proteinase production schemes) hampered the building of such a model.

An important body of modeling work has been carried out about cell–ECM mechanical interactions (DiMilla et al., 1991; Cook et al., 1993; Murray, 1993). Transduction of ECM mechanical characteristics (constraints, deformation, rigidity) to the cell through integrins has been experimentally shown to play a role in cell metabolism (Choquet et al., 1997). The building of a realistic model implies the inclusion in such mechanochemical models of the extracellular proteolysis organization through equations similar to those presented here.

Another limitation of the model presented here is the lack of space representation. Many of the species implicated are soluble and thus diffusive (E, L, or the cell itself). Nevertheless, a recent study about chemotaxis has shown that the solution of the reaction-diffusion equations corresponding to S and L spatial distribution could be traveling waves (Perumpanani et al., 1998). In this case, half of the cells would be found at the intersection between S and L waves, and the spatial terms in the equations locally and monotonically modify S, L, or E concentration. Inasmuch as the diffusion of these species is not accompanied by nonlinear interactions between them, it is not a source of dynamical behavior by itself. Nevertheless, this study also showed that the competition between haptotaxis (cell mobility toward insoluble, substratum-bound attractants: here, S) and chemotaxis (cell motility in response to a gradient of soluble attractant: here, L), can also regulate cell migration. These spatial phenomena (haptotaxis and chemotaxis) should thus also be taken into account in a realistic model.

For simulation purposes, we used a specific protein, Fn, as proteinase substrate. However, the model presented here could be developed in the same way for any integrin-binding ECM protein that presents cryptic functions, such as vitronectin (Bafetti et al., 1998) or laminin (Gianelli et al., 1997). In this case, because the ECM is composed of several of these proteins, which all mediate cell attachment through different integrins, the resulting global variations of [RL] and [RS] would be a superposition of different oscillatory cycles. Cell invasion capacity would therefore be a function of the relative phases of these oscillations, and thus a function of ECM composition and expressed integrins. Depending on the type of ECM encountered, an invasive cell could regulate locomotion by regulating the type and quantity of integrin it expresses. This could partly account for the change in the types of expressed integrins that has often been correlated with the acquisition of invasive phenotypes (Ruoslahti, 1988; Aota et al., 1991; Yao et al., 1997).

REFERENCES

Akiyama, S. K., and K. M. Yamada. 1985. The interaction of plasma fibronectin with fibroblastic cells in suspension. *J. Biol. Chem.* 260: 4492–4500.

Akiyama, S. K., E. Hasegawa, T. Hasegawa, and K. M. Yamada. 1985. The interaction of fibronectin fragments with fibroblastic cells. *J. Biol. Chem.* 260:13256–13260.

Aota, S. I., T. Nagai, K. Olden, S. K. Akiyama, and K. M. Yamada. 1991. Fibronectin and integrin in cell adhesion and migration. *Biochem. Soc. Trans.* 19:830–835.

Assoian, R. K. 1997. Anchorage-dependent cell cycle progression. *J. Cell Biol.* 136:1–4.

Bafetti, L. M., T. N. Young, Y. I. Itoh, and M. S. Stack. 1998. Intact vitronectin induces matrix metalloproteinase-2 and tissue inhibitor of matrix metalloproteinase-2 expression and enhanced cellular invasion by melanoma cells. *J. Biol. Chem.* 273:143–149.

Basbaum, C. B., and Z. Werb. 1996. Focalized proteolysis: spatial and temporal regulation of extracellular matrix degradation at the cell surface. *Curr. Opin. Cell Biol.* 8:731–738.

Birkedal-Hansen, H., W. G. I. Moore, M. K. Bodden, L. J. Windsor, B. Birkedal-Hansen, A. DeCarlo, and J. A. Engle. 1993. Matrix metalloproteinases: a review. *Crit. Rev. Oral Biol. Med.* 4:197–250.

Borchers, A. H., L. A. Sanders, M. B. Powell, and G. D. Bowden. 1997. Melanocytes mediated paracrine induction of extracellular matrix degrading proteases in squamous cell carcinoma cells. *Exp. Cell Res.* 231:61–65.

Bronnikova, T. V., W. M. Schaffer, M. J. B. Hauser, and L. F. Olsen. 1998. Routes to chaos in the peroxidase–oxidase reaction. 2. The fat torus scenario. *J. Phys. Chem. B.* 102:632–640.

Brooks, P. C., S. Strömblad, L. C. Sanders, T. L. von Schalscha, R. T. Aimes, and D. A. Cheresh. 1996. Localization of matrix-metalloproteinase MMP-2 to the surface of invasive cells by interaction with integrin $\alpha V\beta3$. *Cell.* 85:683–693.

Choquet, D., D. P Feslenfeld, and M. P. Sheetz. 1997. Extracellular matrix rigidity causes strengthening of integrin-cytoskeleton linkages. *Cell.* 88:39–48.

Cockett, M. I., G. Murphy, M. L. Birch, J. P. O'Connell, T. Crabbe, A. T. Millican, I. R. Hart, and A. J. P. Docherty. 1998. Matrix metalloproteinases and metastatic cancer. *Biochem. Soc. Symp.* 63:295–313.

Coevoet, M. A., and J. F. Hervagault. 1997. Irreversible metabolic transitions: the glucose 6-phosphate metabolism in yeast cell-free extracts. *Biochem. Biophys. Res. Comm.* 234:162–166.

Cook, J., P. Tracqui, and J. D. Murray. 1993. Mechanochemical models and biological morphogenesis—A brief review. *Forma.* 8:159–178.

Denis, L. J., and J. Verweij. 1997. Matrix metalloproteinase inhibitors: present achievements and future prospects. *Invest. New Drugs.* 15:175–185.

Defilippi, P., M. Venturino, D. Gulino, A. Duperray, P. Boquet, C. Fiorentini, G. Volpe, and G. Tarone. 1997. Dissection of pathways implicated in integrin-mediated actin cytoskeleton assembly. *J. Biol. Chem.* 272:21726–21734.

de Gennes, P. G. 1993. Scaling Concepts in Polymer Physics. Cornell University Press, Ithaca, NY.

DiMilla, P., K. Barbee, and D. A. Lauffenberg. 1991. Mathematical model for the effects of adhesion and mechanics on cell migration speed. *Biophys. J.* 60:15–37.

Fukai, F., T. Iso, K. Sekiguchi, N. Miyatake, A. Tsugita, and T. Katayama. 1993. An amino-terminal fibronectin fragment stimulates the differentiation of ST-13 preadipocytes. *Biochemistry.* 32:5746–5751.

Fukai, F., M. Ohtaki, M. Fujii, H. Yajima, T. Ishii, Y. Nishizawa, K. Miyazaki, and T. Katayama. 1995. Release of biological activities from quiescent fibronectin by a conformational change and limited proteolysis by matrix metalloproteases. *Biochemistry.* 34:11453–11459.

Fukai, F., H. Takahashi, Y. Habu, N. Kubushiro, and T. Katayama. 1996. Fibronectin harbors anticell adhesive activity. *Biochem. Biophys. Res. Comm.* 220:394–398.

Gianelli, G., J. Falk-Marzillier, O. Schiraldi, W. G. Stetler-Stevenson, and V. Quaranta. 1997. Induction of cell migration by matrix metalloprotease-2 cleavage of laminin-5. *Science.* 277:225–228.

Goldbeter, A., and J.-L. Martiel. 1985. Birhythmicity in a model for the cyclic AMP signalling system of the slime mold *Dictyostelium discoideum. FEBS Lett.* 191:149–153.

Goldbeter, A., O. Decroly, Y. X. Li, J.-L. Martiel, and F. Moran. 1988. Finding complex oscillatory phenomena in biochemical systems. An empirical approach. *Biophys. Chem.* 29:211–217.

Goldbeter, A., and J.-M. Guilmot. 1996. Thresholds and oscillations in enzymatic cascades. *J. Phys. Chem.* 100:19174–19181.

Guo, H., S. Zucker, M. K. Gordon, B. P. Toole, and C. Biswas. 1997. Stimulation of matrix metalloproteinase production by recombinant extracellular matrix metalloproteinase inducer from transfected Chinese hamster ovary cells. *J. Biol. Chem.* 272:24–27.

Heino, J. 1996. Biology of tumor cell invasion: interplay of cell adhesion and matrix degradation. *Int. J. Cancer.* 65:717–722.

Homandberg, G. A., F. Hui, C. Wen, C. Purple, K. Bewsey, H. Koepp, K. Huch, and A. Harris. 1997. Fibronectin-fragment-induced cartilage chondrolysis is associated with release of catabolic cytokines. *Biochem. J.* 321:751–757.

Huhtala, P., M. J. Humphries, J. B. McCarthy, P. M. Tremble, Z. Werb, and C. H. Damsky. 1995. Cooperative signaling by $\alpha5\beta1$ and $\alpha4\beta1$ integrins regulates metalloproteinase gene expression in fibroblasts adhering to fibronectin. *J. Cell Biol.* 219:867–879.

Hulboy, D. L., L. A. Rudolph, and L. M. Matrisian. 1997. Matrix metalloproteinases as mediators of reproductive function. *Mol. Human Reprod.* 3:27–45.

Huttenlocher, A., M. K. Ginsberg, and A. F. Horwitz. 1996. Modulation of cell migration by integrin-mediated cytoskeletal linkages and ligand-binding affinity. *J. Cell Biol.* 134:1551–1562.

Huttenlocher, A., S. P. Palecek, Q. Lu, W. Zhang, R. L. Mellgren, D. A. Lauffenburger, and A. F. Horwitz. 1997. Regulation of cell migration by the calcium-dependent protease calpain. *J. Biol. Chem.* 272:32719–32722.

Hynes, R. O. 1983. Fibronectin and its relation to cellular structure and behavior. *In* Cell Biology of Extracellular Matrix. E. D. Hay, editor. Plenum Press, New York. 295–334.

Khan, K. M. F., and D. J. Falcone. 1997. Role of laminin in matrix induction of macrophages urokinase-type plasminogen activator and 92-kDa metalloproteinase expression. *J. Biol. Chem.* 272:8270–8275.

Kindzelskii, A. L., M.-J. Zhou, R. P. Haugland, L. A. Boxer, and H. R. Petty. 1998. Oscillatory pericellular proteolysis and oxidant deposition during neutrophil locomotion. *Biophys. J.* 74:90–97.

Klemke, R. L., S. Cai, P. J. Gallagher, P. de Lanerolle, and D. A. Cheresh. 1997. Regulation of cell mobility by mitogen-activated protein kinase. *J. Cell Biol.* 137:481–492.

LaFlamme, S. E., and K. L. Auer. 1996. Integrin signaling. *Semin. Cancer Biol.* 7:111–118.

Lauffenburger, D. A. 1996. Making connections count. *Nature.* 383:390–391.

Law, D. A., L. Nannizzi-Alaimo, and D. R. Phillips. 1996. Outside-in integrin signal transduction. *J. Biol. Chem.* 271:10811–10815.

Linsenmayer, T. F. 1983. Collagen. *In* Cell Biology of Extracellular Matrix. E. D. Hay, editor. Plenum Press, New York. 5–37.

Liotta, L. A., P. S. Steeg, and W. G. Stetler-Stevenson. 1991. Cancer metastasis and angiogenesis: an imbalance of positive and negative regulation. *Cell.* 64:327–336.

McKeown-Longo, P. J., and D. F. Mosher. 1988. The assembly of the fibronectin matrix in cultured human fibroblast cells. *In* Fibronectin. D. F. Mosher, editor. Academic Press, San Diego, CA. 163–180.

Mikhailov, A., and B. Hess. 1996. Microscopic self-organization of enzymic reactions in small volumes. *J. Phys. Chem.* 100:19059–19065.

Murray, J. D. 1993. Mathematical Biology. Springer Verlag, New York/Berlin.

Nagahara, S., and T. Matsuda. 1996. Cell–substrate and cell–cell interactions differentially regulate cytoskeletal and extracellular matrix protein gene expression. *J. Biomed. Mat. Res.* 32:677–686.

Nakahara, H., L. Howard, E. W. Thompson, H. Sato, M. Seiki, Y. Yeh, and W.-T. Chen. 1997. Transmembrane/cytoplasmic domain-mediated membrane type 1-matrix metalloprotease docking to invadopodia is required for cell invasion. *Proc. Natl. Acad. Sci. USA.* 94:7959–7964.

Palecek, S. P., J. C. Loftus, M. H. Ginsberg, D. A. Lauffenburger, and A. F. Horwitz. 1997. Integrin-ligand binding properties govern cell migration speed through cell-substratum adhesiveness. *Nature.* 385:537–540.

Perumpanani, A. J., D. L. Simmons, A. J. H. Gearing, K. M. Miller, G. Ward, J. Norbury, M. Schneemann, and J. A. Sherratt. 1998. Extracellular matrix-mediated chemotaxis can impede cell migration. *Proc. R. Soc. Lond. B.* 265:2347–2352.

Porter, B. 1967. Stability Criteria for Linear Dynamical Systems. Oliver and Boyd Ltd., London.

Price, J. T., M. T. Bonovich, and E. C. Kohn. 1997. The biochemistry of cancer dissemination. *Crit. Rev. Biochem. Mol. Biol.* 32:175–253.

Ruoslahti, E. 1988. Fibronectin and its receptors. *Ann. Rev. Biochem.* 57:375–413.

Schlaepfer, D. D., and T. Hunter. 1997. Focal adhesion kinase overexpression enhances Ras-dependent integrin signaling to ERK2/mitogen-activated protein kinase through interactions with and activation of c-Src. *J. Biol. Chem.* 272:13189–13195.

Sobolev, S. L. 1989. Partial Differential Equations of Mathematical Physics. T. A. A. Broadbent, editor. English translation by E. R. Dawson. Dover Publications, Inc., NY.

Sudbeck, B. D., B. K. Pilcher, H. G. Welgus, and W. C. Parks. 1997. Induction and repression of collagenase-1 by keratinocytes is controlled by distinct components of extracellular matrix. *J. Biol. Chem.* 272: 22103–22110.

Tamura, M., J. Gu, K. Matsumoto, S.-I. Aota, R. Parsons, and K. A. Yamada. 1998. Inhibition of cell migration, spreading and focal adhesions by tumor suppressor PTEN. *Science.* 280:1614–1617.

Taylor, K. B., L. J. Windsor, N. C. M. Caterina, M. K. Bodden, and J. A. Engler. 1996. The mechanism of inhibition of collagenase by TIMP-1. *J. Biol. Chem.* 271:23938–23945.

Ugarova, T. P., A. V. Ljubimov, L. Deng, and E. F. Plow. 1996. Proteolysis regulates exposure of the IIICS-1 adhesive sequence in plasma fibronectin. *Biochemistry.* 35:10913–10921.

Vassali, J. D., and M. S. Pepper. 1994. Membrane proteases in focus. *Nature.* 370:4–15.

Werb, Z., P. M. Tremble, O. Behrendtsen, E. Crowley, and C. Damsky. 1989. Signal transduction through the fibronectin receptor induces collagenase and stromelysin gene expression. *J. Cell Biol.* 109:877–889.

Werb, Z. 1997. ECM and cell surface proteolysis: regulating cellular ecology. *Cell.* 91:439–442.

Wu, C. 1997. Roles of integrins in fibronectin matrix assembly. *Histol. Histopathol.* 12:233–240.

Xiao, Y., and G. A. Truskey. 1996. Effect of receptor-ligand affinity on the strength of endothelial cell adhesion. *Biophys. J.* 71:2869–2884.

Xie, D.-L., and G. A. Homandberg. 1993. Fibronectin fragments bind to and penetrate cartilage tissue resulting in proteinase expression and cartilage damage. *Biochim. Biophys. Acta.* 1182:189–196.

Yamada, K. M. 1997. Integrin signaling. *Matrix Biol.* 16:137–141.

Yao, M., X. D. Zhou, X. L. Zha, D. R. Shi, J. Fu, J. Y. He, H. F. Lu, and Z. Y. Tang. 1997. Expression of the integrin $\alpha5$ subunit and its mediated cell adhesion in hepatocellular carcinoma. *J. Cancer Res. Clin. Oncol.* 123:435–440.

Yebra, M., G. C. N. Parry, S. Strömblad, N. Mackman, S. Rosenberg, B. Mueller, and D. A. Cheresh. 1996. Requirement of receptor-bound urokinase-type plasminogen activator for integrin $\alpha V\beta5$-directed cell migration. *J. Biol. Chem.* 271:29393–29399.